RSC Applied Interfaces

ROYAL SOCIETY OF CHEMISTRY

PAPER

View Article Online
View Journal | View Issue

Cite this: *RSC Appl. Interfaces*, 2024, **1**, 1036

A closer examination of white-rot fungal mycelia assisted wood bonding†

Wenjing Sun, *[ab] Islam Hafez,[bc] Barbara J. W. Cole[d] and Mehdi Tajvidi[b]

Received 23rd February 2024,
Accepted 5th May 2024

DOI: 10.1039/d4lf00061g

rsc.li/RSCApplInter

This study investigated the adhesion at the interface between mycelium and wood in detail, focusing on the evaluation of different bonding systems and the influence of hot-pressing temperature on bonding strength. The behavior of water-soluble components and their significance in this context were examined through chemical extraction experiments and analysis. The results indicated that both degraded wood veneer and surface mycelium exhibit comparable bonding strength. In addition, a significant finding of the study is that water-soluble components washed from mycelium, which exhibit a 7% higher protein content and a distinct carbohydrate composition compared to those washed from wood, are crucial in achieving effective bonding. Notably, proteins and high-molecular-weight carbohydrates are identified as key factors responsible for the favorable bonding behavior observed with mycelium. These findings offer valuable insights for the further development of sustainable materials utilizing mycelium as a binder and emphasize the importance of manipulating the composition of water-soluble components to optimize interfacial adhesion.

Introduction

Over the past few years, there has been a significant push towards developing sustainable, nature-based materials to replace petroleum-derived products in order to achieve carbon-neutrality.[1–3] Lignocellulosic biomass, predominantly wood, has been used throughout human history due to its abundance, versatility, and low cost. However, the adhesives used traditionally to bond wood-based composites are usually unsustainable and have been a major concern attributed to their environmental implications and sourcing from petroleum.[4,5] Thus, both industry and academia are making efforts to generate processes and products that are more sustainable. For example, by 2030, IKEA has set targets to decrease the use of fossil-based adhesives by 40%, reduce the climate impact of adhesives by 30%, and ensure that most factories producing boards in its supply chain employ adhesives with lower climate impacts.[6]

Fungal mycelium is a unique candidate for bio-based adhesives.[7] The way it binds lignocellulosic biomass is distinctive. It grows and penetrates the substrate, acting not only as a binder but also as a fiber-like structure that reinforces the entire structure. Alongside the environmental benefits such as biodegradability, renewability, and a low carbon footprint, mycelium-bound products also demonstrate scalability potential. Several companies have already successfully scaled up the production of these products, such as construction panels, packaging, acoustic and thermal insulation foams, and more.[8,9] However, the adhesion details at the interface and their influence on the properties of the composites are still unclear due to the complexity of both materials, which primarily include cellulose, hemicelluloses, lignin, extractives in lignocellulosic biomass, and chitin, glucan, and proteins in hyphae.[7,10,11]

Previous research has demonstrated the significance of the mycelium–wood interface in bonding wood veneer.[10] This interface marks the bottom surface of the mycelium and the top surface of the wood veneer. The adhesion potential of the mycelium layer's bottom surface can support a single mycelium layer to bond untreated wood, while the modified wood surface can also provide impressive bonding to the wood veneers themselves without any mycelium.[10] Moreover, the bonding strength of mycelium-bonded wood was comparable to that of commercial wood glue, with the mycelium adhesive demonstrating better resilience to water exposure.[10] The adhesion at the interface is thought to be associated with enzymes secreted by fungi, degraded wood components such as monosaccharides, and depolymerized lignin, through mechanisms including diffusion, hydrogen bonding, and potential covalent bonding after heat treatment. However, these theories are yet to be fully confirmed, and several remaining

[a] *Institute of Materials (IMX), École Polytechnique Fédérale de Lausanne (EPFL), Lausanne 1015, Switzerland. E-mail: wenjing.sun@epfl.ch*
[b] *Laboratory of Renewable Nanomaterials, School of Forest Resources, University of Maine, Nutting Hall, Orono, Maine 04469-5755, USA*
[c] *Department of Wood Science and Engineering, Oregon State University, Corvallis, Oregon 97331, USA*
[d] *Department of Chemistry, University of Maine, Orono, Maine, 04469-5755, USA*
† Electronic supplementary information (ESI) available. See DOI: https://doi.org/10.1039/d4lf00061g

questions exist. For instance, how much of the "adhesion components" attach to the mycelium bottom surface and how much remains on the veneer surface when separating surface mycelium from wood veneer surface, and how do they contribute to the bonding of stand-alone mycelium and stand-alone wood? What are the adhesion mechanisms involved in different systems, and what is the extent of their contributions? How does the change in the pressing temperature influence bonding performance, and how stable is adhesion in wet conditions?

To address these questions, we aimed to further investigate the mycelium–wood interface. In this work, we started by testing three bonding systems: "degraded veneer without surface mycelium", "degraded veneer with surface mycelium", and "untreated veneer with surface mycelium". We evaluated the effect of hot-pressing temperature on both dry and wet lap-shear strength of the wood veneer samples. We also examined the importance of water-soluble components in these systems by washing the separated veneer and mycelium with water separately and evaluating changes in their adhesion behavior. Finally, we identified the chemicals that had been washed off from veneer and mycelium and the changes on the surfaces, providing us with a better understanding of the adhesion details at the interface of fungal mycelium and lignocellulosic biomass.

Results and discussion

Adhesion performance

Fig. 1 shows the adhesion performance of the three major groups: "degraded veneer without surface mycelium" (D), "degraded veneer with surface mycelium" (DM), and "untreated veneer with surface mycelium" (UM), where the degradation times were all 15 days. Generally, the dry lap-shear strength (Fig. 1A and C) followed the trend we observed previously.[10] The DM group showed the highest strength in all three temperatures examined. Groups D and UM also showed competitive dry lap-shear strengths, and exhibited little or no difference with the DM group at 120 °C and 180 °C temperatures. There was no significant difference ($p > 0.05$) between the D and UM groups at any of the three temperatures (as indicated by the shared letters above the respective bars in the figures), indicating that stand-alone degraded veneer and stand-alone mycelium sheets had similar adhesion potential. However, they behaved very differently after water washing. As shown in Fig. 1A and C, after water washing (WD group), the D group did not lose any of its dry lap-shear strength (Fig. 1A); the results at all three temperatures exhibit no significant difference ($p > 0.05$) compared to the unwashed group. As for the UM group, however, after washing (WUM group), the surface mycelium layer lost most of its bonding strength at all three press temperatures examined. This indicates that the water-soluble components that had been washed off were essential for mycelium bonding but not necessary for wood bonding.

Fig. 1B and D show the wet lap-shear strength of different groups after being soaked in water for 48 h. Water-resistance properties are essential for exterior applications and can provide useful information on the adhesion mechanism. As expected, all the groups lost more than 70% of their lap-shear bonding strength. For 120 °C pressed D and WD groups, all the samples were delaminated after soaking in water for 48 h; therefore, no data could be obtained. There

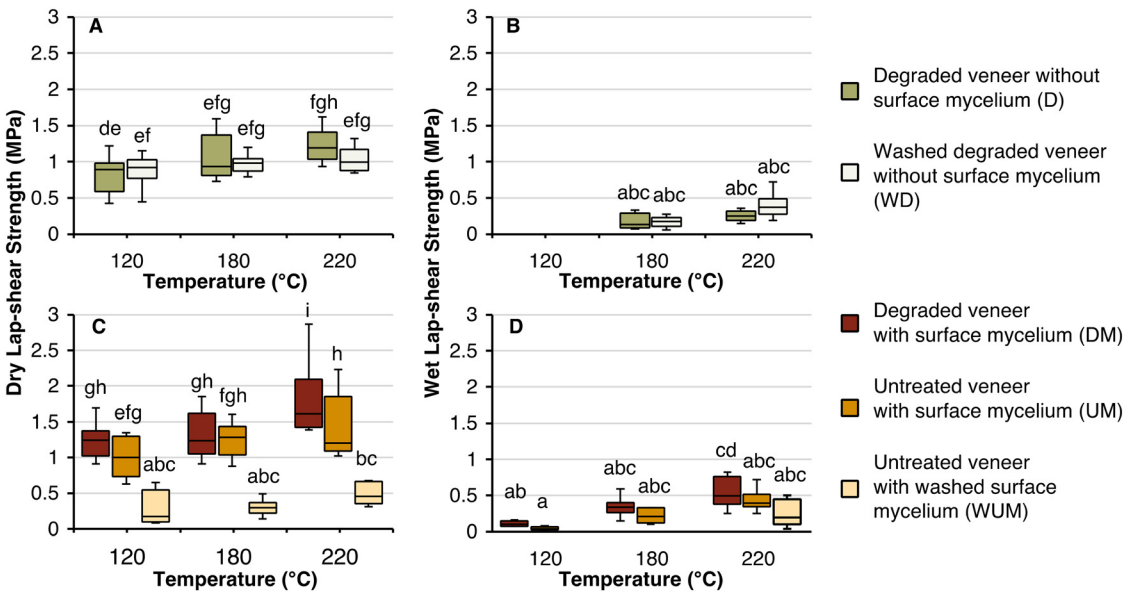

Fig. 1 Lap-shear strengths of different samples after different temperature hot-pressing tested under variable conditions. (A) Unwashed and washed degraded veneer, dry strength; (B) unwashed and washed degraded veneer, wet strength; (C) degraded veneer with surface mycelium, untreated veneer with unwashed or washed surface mycelium, dry strength; (D) degraded veneer with surface mycelium, untreated veneer with unwashed or washed surface mycelium, wet strength. Data points with common letters are not significantly different at 95% confidence level ($p > 0.05$).

was no significant difference ($p > 0.05$) in the strength value between 180 °C and 220 °C pressed WD groups and they were all lower than 0.5 MPa (Fig. 1B). The wet lap-shear strength of the DM and UM groups behaved similarly; only the DM group that was pressed at 220 °C showed a value slightly higher than the other groups (0.54 MPa) but not significantly different ($p > 0.05$) (Fig. 1D).

From a practical point of view, it seems that there is no need to apply a higher temperature for better bonding. As for all three systems, only increasing the hot-pressing temperature from 120 °C to 220 °C was able to achieve some but still very little improvement in the lap-shear strength. And the wet strength for all the temperatures was very low, which will limit the applications for the products that purely rely on these bonding systems. These observations are different from some previous research, where higher temperatures generally showed higher MOR values for composite products.[11] However, none of the studies compared the temperature in the same experimental set-up; the trend might just be caused by other experimental factors such as the composite type, the pressure and time used, or substrate species.

As for the adhesion mechanism examination, the weak wet strength indicates that there are not enough covalent bonds in the adhesion system. The bonding may come from water-sensitive hydrogen bonds and van der Waals interactions.[12] Increasing the pressing temperature may degrade more surface components to small molecules and accelerate their softening and flow to improve the diffusion and mechanical interlocking,[13] but this was not very efficient in our experimental set-up.

Wood veneer analysis

Fig. S1† illustrates the thickness compression of autoclaved and degraded veneer samples after hot pressing at various temperatures. The degraded veneer samples show less bulk thickness compression compared to the autoclaved veneers. This lesser compression in the degraded samples is indicative of a less compact structure, including the surface, which may negatively impact the formation of effective mechanical interlocks, a key aspect of mechanical interlocking adhesion theory. Additionally, it is important to note that the initial thickness of the degraded veneers was approximately 9% less than that of the autoclaved ones. This difference in starting thickness may have influenced the extent of compression observed, potentially affecting the comparability and interpretation of mechanical interlocking efficiency between the two sets of samples. Given these observations, it appears that mechanical interlocking may not be the predominant factor contributing to the increase in bonding strength of veneers after fungal degradation.

The chemical changes of the veneer surfaces as a result of fungal degradation are shown in Fig. 2. The fingerprint areas of the FTIR spectra (Fig. 2A) show no major changes after degradation and washing, indicating that the chemical components remained similar on the surface or that any small differences could not be detected using FTIR. With the increase of hot-pressing temperature, the two peaks at 1594 cm^{-1} and 1640 cm^{-1}, representing the aromatic rings of lignin, became closer and merged at 220 °C. This may be attributed to the increase in relative lignin content attributable to the degradation of hemicellulose.[14] In contrast, the peaks between 1460 and 1470 cm^{-1}, attributed to aliphatic CH bending of lignin, were separated into two peaks after heat treatment. This separation may indicate lignin undergoing changes, potentially due to either condensation or the formation of CH_2 bridges between lignin fragments.[14] The peak at 1250 cm^{-1} was relatively increased in intensity and separated into two peaks, indicating new linkages on the asymmetric C–O–C stretching band for lignin.[15] The appearance of the peak at 781 cm^{-1} also could be attributed to changes in lignin or reveals the production of new unknown compounds after high-temperature treatment.[16]

XPS was also applied on the veneer surfaces after different treatments (Fig. 2B–D) to study the surface chemistry changes. As shown in Fig. 3B and C, the relative O/C and N/C ratios were increased after degradation and decreased after hot-pressing. The increase after degradation indicates the oxidation of the veneer surface and the secreted proteins from fungi.[17] The decrease in O/C ratio with the heating process (Fig. 2B) could be attributed to hemicellulose degradation and lignin rearrangement during the heat treatment as the O/C ratio of hemicellulose is much higher than that of lignin.[18] Fig. 2D shows the percentage of different carbon types. Carbon I corresponds to carbon atoms bonded only to carbon or hydrogen atoms (C–H, or C–C); carbon II corresponds to carbon atoms bonded to one single non-carbonyl oxygen atom (C–O); and carbon III peak corresponds to carbon atoms bonded to a carbonyl or two non-carbonyl oxygen atoms (C═O or O–C–O).[18,19] The degradation of wood veneer caused the decrease of carbon I and the increase of carbon III (Fig. 2D), confirming the oxidation caused by fungal degradation. Carbon I further decreased after heat treatment, which may be attributed to the reactions of fragmentation and oxidation because of the high temperature. The increase of carbon II at 220 °C may be due to the degradation of amorphous polysaccharides and the general increase of carbon II is due to the formation of carbonyl structures.[20]

FTIR and XPS spectra differences between different groups suggested that chemical transformations occurred on the veneer surface leading to the formation of new chemical bonds after the degradation by hot-pressing, which may contribute to the bonding.

Supernatant analysis

One intriguing finding from the lap-shear tests was the significant contribution of water-soluble components washed off from the surface mycelium layer in bonding untreated wood veneers. To quantify these components, we freeze-dried the washed-off liquids and measured the mass to calculate

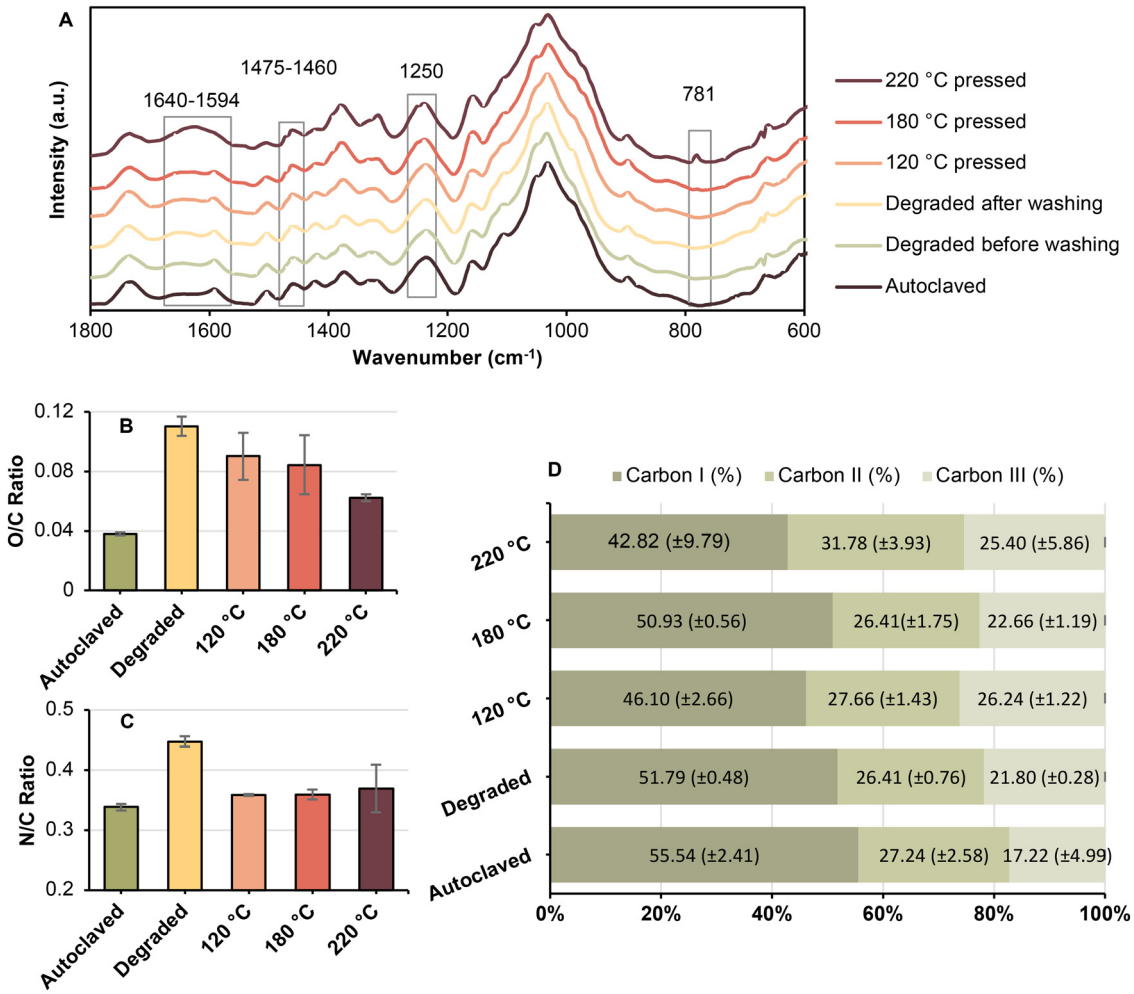

Fig. 2 Chemical changes of wood veneers after degradation, washing and hot-pressing. (A) FTIR; (B) O/C ratio; (C) N/C ratio; (D) carbon I, II, III ratios.

the yield of the water-soluble compounds per piece of veneer. The yield from the supernatants washed from veneer (SV) was 2.38 (±0.27)% and from the supernatants washed from mycelium (SM), notably higher at 10.37 (±0.16)%. In order to ascertain their role, we re-dissolved the freeze-dried components in water and utilized them as adhesives to evaluate their bonding properties.

Fig. 3A shows the dry lap-shear strength of autoclaved wood veneers bonded with SV and supernatants washed from mycelium SM and hot-pressed at 120 °C. Notably, SV-bonded untreated veneers showed similar strength to bonded unwashed (D) and washed degraded (WD) veneers (Fig. 1A). Differently, SM showed a much higher lap-shear bonding strength (Fig. 3A), 2.22 MPa. It is significantly higher than the values of all groups pressed at 120 °C (Fig. 1A and C) and confirms the importance of water-soluble components in the bonding system of the surface mycelium layer.

The chemical compositions of SV and SM were characterized to further understand the difference in their origin, structure, and adhesion behavior. The FTIR spectra of SV revealed typical peaks at 1730, 1604, 1509, 1381, and 1250 cm^{-1}, indicating that SV compositions include hemicellulose and lignin fractions (Fig. 3C).[21,22] The FTIR spectrum (Fig. 3C) of SM shows similar peaks to SV with some differences. The missing peak at 1730 cm^{-1}, which corresponds to the carbonyl group, indicates that the degraded xylan fractions mostly remained in the wood veneers. The peak at around 1620 cm^{-1} (amide I: C═O, C–N) is broader and there are two more peaks appearing at 1545 cm^{-1} (amide II: C–N, C–H) and 1317 cm^{-1} (amide III: CO–NH) compared with the veneer supernatant, which indicates that more protein exists in the mycelium supernatant.

The protein concentration analysis indicates a 7% higher protein content in SM compared to SV (Fig. 3C). ^{13}C NMR spectra also support this finding, revealing substantial amounts of proteins in both samples, as evidenced by the presence of ^{13}C chemical shifts in the carbonyl, aromatic, and aliphatic regions (Fig. S3†). Moreover, the ratio between carbonyl C and sugar anomeric C is significantly higher in SM than SV.

Glycosyl analysis demonstrates a significant difference in xylose content, with SV containing 29% xylose (Xyl) compared to only 7% in SM (Fig. 3D). The elevated level of xylose in SV may

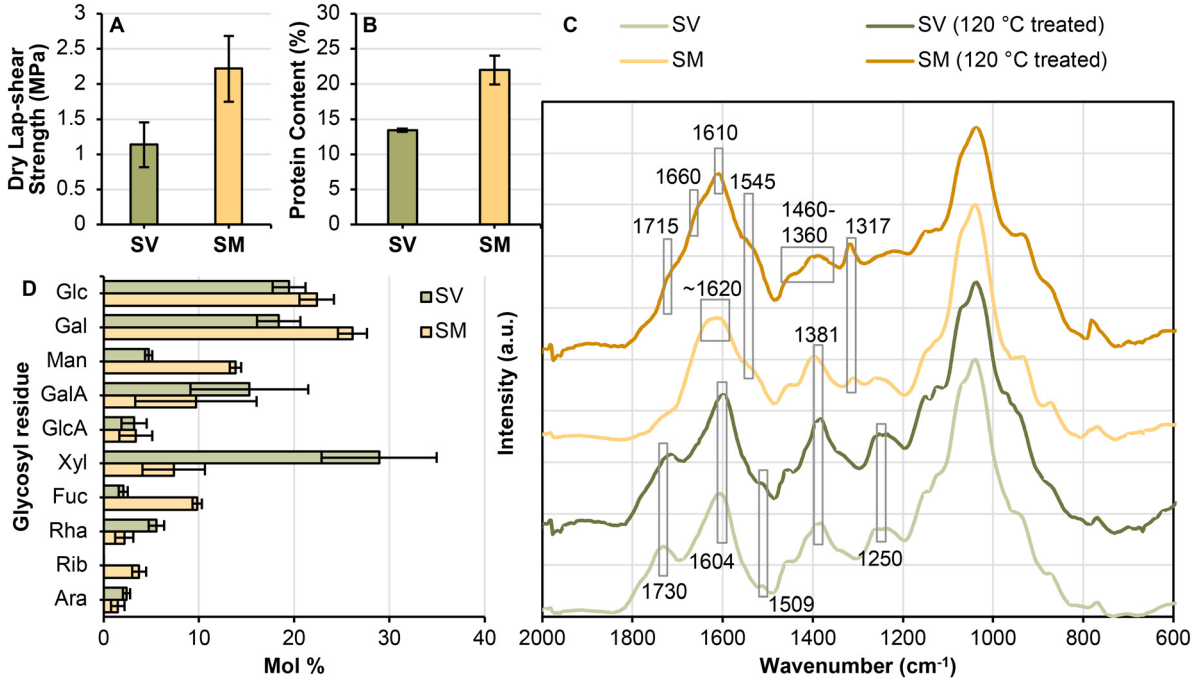

Fig. 3 Performance and characterization of freeze-dried supernatants from veneer (SV) and mycelium (SM): (A) dry lap-shear strength; (B) protein content; (C) FTIR; (D) monosaccharide compositions.

be due to the intensive degradation of the main polymer chain and the inherent solubility of birch xylan, which is characteristically acetylated and contains glucuronic acid side chains. Additionally, dominant monosaccharides identified in SV included glucose (Glc) at 19%, galactose (Gal) at 18%, and galacturonic acid (GalA) at 15%, all are common components of birch hemicellulose,[23] confirming the degradation of hemicellulose. The presence of high levels of Glc suggests the degradation of cellulose. Previous studies have shown that monosaccharide composition varies during degradation, with side-chain elements being more susceptible to degradation compared to the main polymer chain.[23,24] Therefore the degradation might be intensive at this particular stage. Differently, major monosaccharides identified in SM are Gal at 26%, Glc at 22%, and mannose at 14%. Water-soluble components from fungal mycelium are believed to mainly consist of extracellular polysaccharides (EPS), typically extracted from the supernatant of liquid fermentation.[25,26] In solid-state fermentation, such as in our case, the EPS accumulates and forms a matrix around the hyphae at the interface between the substrate and the mycelium (so-called biofilm hyphae in some contexts).[10,27] The dominant monosaccharides detected in SM align with the reported EPS composition of *Basidiomycetes* from liquid fermentation, which varies with species, growing conditions, and additives, but most of them contain glucose, mannose, and galactose, which are the dominant monosaccharides in the SM sample.[25] The SEC chromatograms (Fig. S3†) reveal that the major components in both SV and SM have an average molecular weight of 1 kDa. However, SM contains additional minor components in the range of 1050 kDa, 100 kDa, 60 kDa, and 20 kDa, absent in SV, supporting the presence of EPS in SM. Further analysis shows that SM includes a higher proportion of higher-molecular-weight components compared to SV (Fig. S3B†), which may relate to the fact that their adhesion ability is higher.

Referring back to Fig. 3C, the FTIR curve of SV shows no significant changes after heat treatment, while SM exhibits some changes. SM displays a broad peak at the region around 1620 cm^{-1}, which corresponds to amide II of the proteins. After heat treatment, it shifts to the wavelength of 1610 cm^{-1} as a sharp peak, which along with the increased intensity of the amide III peak at 1317 cm^{-1}, may indicate protein denaturation and conformation change due to heat treatment.[28] There is also some evidence of Maillard-related reactions between proteins and reducing sugars after heat treatment of the mycelium supernatant. The peak at 1660 cm^{-1} has been assigned to the C═N stretching vibration, indicating Schiff's base products.[29] The appearance of an additional frequency shoulder at 1715 cm^{-1}, corresponding to a carbonyl (C═O) group, may originate from the Amadori products (glycated residues).[28] The features between 1360 and 1460 cm^{-1} are broader after heat treatment, probably corresponding to the C–N═C bonds of imines.[28,30] Similarly, in the ^{13}C NMR spectrum, after heat treatment, only subtle changes occurred in SV, whereas the protein signal region of SM became broader, suggesting conformational changes in the protein structure (Fig. S2†).

It is important to note that the components that had been washed off (SV and SM) were not solely located at the interface between the top surface of the wood veneer and the bottom surface of the mycelium layer. Since the entire veneer and mycelium sheet were washed in water, water-soluble components were extracted from all thickness levels. Therefore,

SV should include components from penetrative mycelial hyphae inside wood; and some degraded wood components may also be attached to the mycelium sheet and may have been included in the analysis of SM. Additionally, after freeze-drying, both SV and SM contained insoluble fractions, which may introduce variations in analysis. However, our previous studies have demonstrated that the bottom surface of the mycelium layer exhibits significantly higher bonding strength compared to the top surface;[10] and the lap-shear strength results of this work clearly indicated the importance of SM in bonding. Thus, we believe our investigation is heading in the right direction and holds considerable significance. The findings of this study reveal that water-soluble components, comprising approximately 22% proteins, with a substantial proportion of small molecular weight carbohydrates and a small fraction of large molecular weight carbohydrates, contribute significantly to fungal-assisted wood bonding. In the bonding systems that rely on the interface, such as plywood and laminated veneers, it will be beneficial to explore approaches to enhance these materials through increasing the water-soluble components, such as changing the growing environment, selecting suitable species or engaging in gene modification. For more complex systems such as mycelium-bonded composites, additional factors such as the structure and quality of the mycelial hyphae themselves also need to be taken into consideration when optimizing the interfacial adhesion.

In the kinetic exploration of adhesion mechanisms, as outlined in Fig. 4, we observed that wood–wood bonding does not primarily rely on the mechanical interlocking of wood cells. Instead, it suggests a more complex interaction, likely involving chemical transformations due to degradation and heat, such as the diffusion of softened lignin and covalent bonding through lignin condensation. Conversely, wood–mycelium bonding is markedly influenced by water-soluble components containing carbohydrates and proteins, which diffuse into the porous structure and may form covalent bonds *via* the Maillard reaction. Both bonding types seem to reach their optimal effectiveness at a pressing temperature of 120 °C, with limited additional improvement at higher temperatures. However, the diminished wet strength in both systems suggests that the predominant bonding mechanisms are hydrogen bonds and van der Waals interactions, resulting from the redistribution of surface components.

Experimental section

Materials

Yellow birch (*Betula alleghaniensis* Britt.) wood veneers with a thickness of 0.61 (±0.04) mm were kindly supplied by Columbia Forest Products LLC (Presque Isle, ME). The chemical composition of the veneer, as determined by NREL

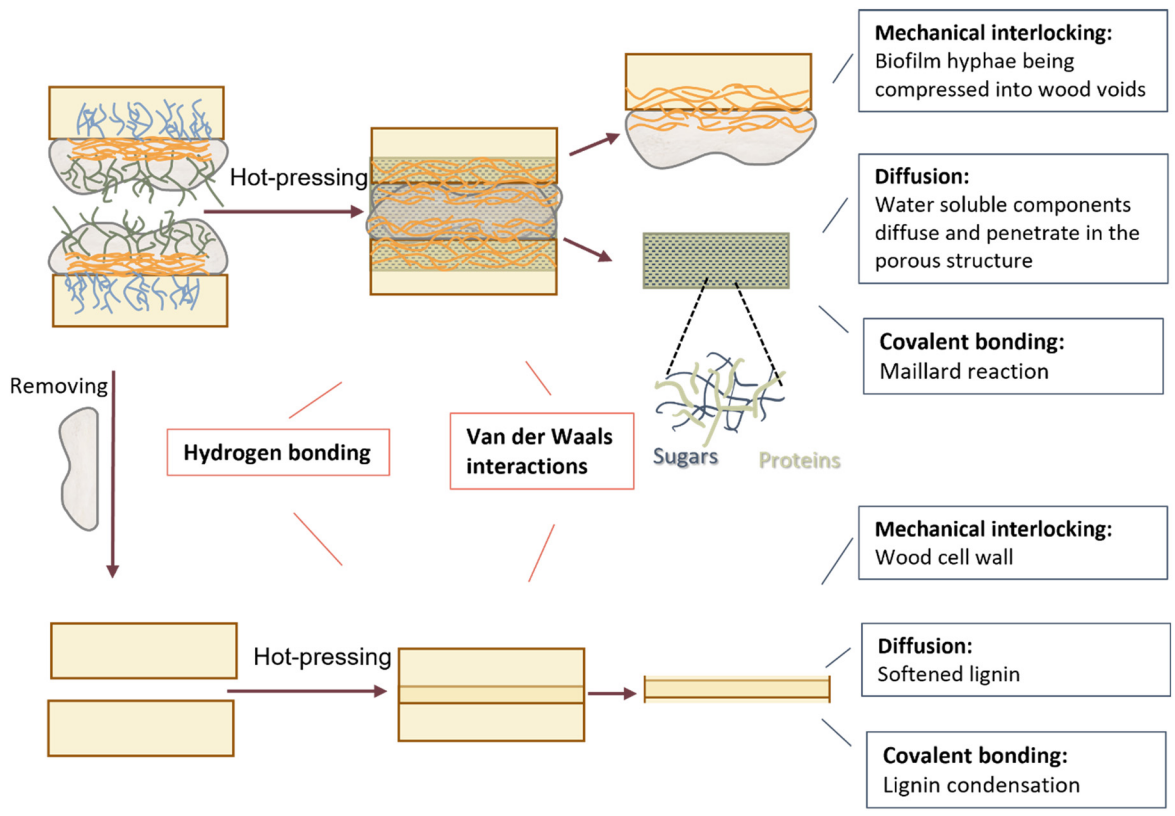

Fig. 4 Schematic figure showing adhesion mechanisms involved in wood–wood bonding and wood–mycelium bonding in view of current adhesion theories.

standards,[31–33] comprises cellulose at 44%, hemicellulose at 29%, lignin at 26%, ash at 0.4%, and extractives at 0.6%. *Trametes versicolor* that had been maintained on agar plates at 4 °C and was pre-incubated on malt extract agar (MEA) plates before the incubation process was supplied by Ecovative Design LLC (Green Island, NY).

Mycelium incubation

The incubation methods were modified from the literature.[34] Yellow birch veneer samples with the dimensions of 80 mm (length) × 80 mm (width) were steam sterilized at 121 °C for 60 min and soaked for about five seconds in 2% (w/v) corn steep liquor (CSL) (Sigma-Aldrich, Saint Louis, MO) containing suspended fungal mycelium. One MEA plate overgrown by the fungus was mixed in 150 mL 2% (w/v) sterile CSL in a BagMixer (Interscience, St Nom, France) for 3 min and transferred to Petri dishes containing MEA. A plastic canvas mesh was used as support between the veneer and agar. The Petri dishes were incubated at 28 °C, 80% relative humidity (RH) for 15 days.

Hot-press and lap-shear samples preparation

After incubation, the wood veneers were cut into strips of 40 mm × 20 mm before hot pressing. Samples were prepared in three ways: 1) the surface mycelium was entirely removed, 2) the surface mycelium was maintained in the bonding area (20 mm × 10 mm), or 3) the separated mycelium layer was applied between two undegraded strips of veneer in the same configuration as the original degraded samples. For the water-washed veneer and mycelium samples, the separated veneer and mycelium pieces were put in a bag filled with deionized water (100 mL per piece). The sealed bags were taped on a plate shaker (VWR Scientific Products rocking platform model 100, Radnor, PA, USA) and were shaken at full speed for 2 h. The washed samples were directly used for hot-pressing and the supernatant was freeze-dried for further analysis. The lap-shear samples were hot-pressed for 5 min (Carver, INC., Wabash, IN, USA). The moisture content of the veneer and mycelium samples before hot-pressing were around 58% and 89%, respectively. Different hot-pressing temperatures (120, 160, and 180 °C) were applied to different groups. The pressure was controlled at 2.78 MPa. Slight densification of wood veneers under this pressure could be expected but this was the lowest manageable pressure to apply using our hot press and it was kept constant for all experiments. The freeze-dried supernatant was diluted in water and applied to the wood veneers as a binder (50 wt%, 10 mg cm^{-2} per glueline) for comparison.

Lap-shear strength test

The lap-shear tests were conducted on an Instron 5942 (Instron, Norwood, MA, USA) with a 500 N capacity load cell. The hot-pressed samples were conditioned at 23 ± 2 °C and 50 ± 2% RH for 48 h (adequate to reach a constant mass). The crosshead speed was 0.5 mm min^{-1}, and the initial gauge length was 40 mm. Twelve replicates were tested for each group. Wet strength tests were carried out by soaking bonded samples in distilled water at room temperature 23 ± 1 °C for 48 h and testing immediately.

X-ray photoelectron spectroscopy (XPS)

The XPS analysis was conducted with a hemispherical energy analyzer (SPECS PHOIBOS HSA 3000 Plus). The X-ray radiation was induced by an aluminum anode. For each group, two replicates were measured.

Attenuated total reflection-Fourier transform infrared spectroscopy (ATR-FTIR)

ATR-FTIR spectra of the surfaces were obtained using a Spectrum Two IR spectrometer (Perkin Elmer, Waltham, MA). All spectra were obtained in the range from 4000 to 600 cm^{-1} with 4 cm^{-1} resolution, accumulating 64 scans. The samples were all tested in room temperature. To ensure the reproducibility of the obtained spectra, three replicates were measured.

Protein concentration

The protein concentration of freeze-dried supernatants was determined using a modified Lowry protein assay kit (Pierce Biotechnology, IL). The proteins were precipitated with acetone and redissolved in deionized water to remove potential interfering substances.

Glycosyl composition analysis

Glycosyl composition analysis was performed, with minor modifications, by gas chromatography-mass spectrometry (GC-MS) of the per-*O*-trimethylsilyl (TMS) derivatives of the monosaccharide methyl glycosides generated from the samples by HCl methanolysis as described previously.[35] A 1 mg portion of each sample was weighed and dissolved in nanopure water to a final concentration of 10 mg mL^{-1}. A 40 μL (400 μg) aliquot of each sample was transferred into a glass screw-top tube, and 20 μg of inositol was added as internal standard. Each sample was heated in 2 N trifluoroacetic acid (TFA) in a sealed screw-top glass test tube for 2 h at 120 °C. After drying under nitrogen flow, each hydrolysate was heated in 1 M methanolic HCl for 18 h at 80 °C. After cooling and removal of the solvent under a stream of nitrogen, each sample was treated with a mixture of methanol, pyridine, and acetic anhydride for 30 min for *N*-acetylation. The solvents were evaporated, and each sample was derivatized with Tri-Sil™ HTP Reagent (Thermo Scientific) at 80 °C for 30 min. GC-MS analysis of the TMS methyl glycosides was performed on an Agilent 7890A GC interfaced to a 5957C mass selective detector (MSD), using a Supelco Equity-1 fused silica capillary column (30 m × 0.25 mm internal diameter (ID)).

Statistical analysis

The obtained lap-shear strength values were analyzed using one-way analysis of variance (ANOVA) to determine statistical differences between the means. A Tukey's honestly significant difference (HSD) multiple comparison test was then performed to further assess the significance level of the mean values for each treatment level. All comparisons were made at a 95% confidence level. All the analyses were performed using RStudio (version 1.2.5033).

Conclusions

In conclusion, our investigation revealed that both degraded wood veneer and surface mycelium demonstrate similar bonding strength when hot-pressed at 120 °C. The specific composition of proteins and carbohydrates within the water-soluble components of mycelium plays an essential role in facilitating adhesion. This study contributes to our understanding of white-rot fungal mycelium-assisted wood bonding, highlighting the potential of fungal mycelia as a sustainable binder and emphasizing the necessity of optimizing water-soluble components to improve interfacial adhesion in sustainable material development.

Author contributions

WS: conceptualization, data curation, formal analysis, methodology, writing – original draft, writing – review & editing, visualization. IH: conceptualization, data curation, formal analysis, methodology, writing – original draft, writing – review & editing. BJWC: conceptualization, methodology, supervision, writing – review & editing. MT: conceptualization, funding acquisition, project administration, resources, supervision, writing – review & editing.

Conflicts of interest

There are no conflicts to declare.

Acknowledgements

The work is supported by the US. Department of Agriculture's Agricultural Research Service (USDA ARS Agreement No. 58-0204-003). The authors thank Ecovative Design LLC for providing the mycelium culture and Columbia Forest Products LLC for providing wood veneers. The authors thank Ayan Dutta, Drs. William Gramlich, Karl Bishop, Douglas Gardner, and Christopher G. Hunt for their scientific support and advice. The authors wish to acknowledge the contributions of Li Tan, Christian Heiss, and Parastoo Azadi in the characterization samples provided by GlycoMIP, a National Science Foundation Materials Innovation Platform funded through Cooperative Agreement DMR-1933525.

References

1 ICYMI, https://www.whitehouse.gov/ceq/news-updates/2021/12/13/icymi-president-biden-signs-executive-order-catalyzing-americas-clean-energy-economy-through-federal-sustainability/, (accessed July 3, 2023).
2 *European Climate Law*, https://climate.ec.europa.eu/eu-action/european-green-deal/european-climate-law_en, (accessed July 3, 2023).
3 N. Stern, *Journal of Government and Economics*, 2022, **6**, 100036.
4 G. I. Mantanis, E. Th. Athanassiadou, M. C. Barbu and K. Wijnendaele, *Wood Mater. Sci. Eng.*, 2018, **13**, 104–116.
5 O. US EPA, *Formaldehyde Emission Standards for Composite Wood Products*, https://www.epa.gov/formaldehyde/formaldehyde-emission-standards-composite-wood-products, (accessed July 3, 2023).
6 *IKEA to use bio-based glue for reduced climate footprint*, https://about.ikea.comhttps://about.ikea.com/en/newsroom/2023/03/01/ikea-to-use-bio-based-glue-for-reduced-climate-footprint, (accessed May 2, 2023).
7 W. Sun, M. Tajvidi and C. G. Hunt, in *Biobased Adhesives*, John Wiley & Sons, Ltd, 2023, pp. 463–475.
8 W. Sun, *Biointerphases*, 2024, **19**, 018502.
9 E. Peeters, J. Salueña Martin and S. Vandelook, *BioChem*, 2023, **45**, 8–13.
10 W. Sun, M. Tajvidi, C. Howell and C. G. Hunt, *ACS Appl. Mater. Interfaces*, 2020, **12**, 57431–57440.
11 W. Sun, M. Tajvidi, C. G. Hunt, B. J. W. Cole, C. Howell, D. J. Gardner and J. Wang, *J. Cleaner Prod.*, 2022, **353**, 131659.
12 D. J. Gardner, in *Characterization of the Cellulosic Cell Wall*, ed. D. D. Stokke and L. H. Groom, Blackwell Publishing Professional, Ames, Iowa, USA, 2006, pp. 254–265.
13 M. A. Hubbe, A. Pizzi, H. Zhang and R. Halis, *BioResources*, 2018, **13**, 2049–2115.
14 B. Belleville, T. Stevanovic, A. Cloutier, A. P. Pizzi, M. Prado, S. Erakovic, P. Diouf and M. Royer, *Eur. J. Wood Wood Prod.*, 2013, **71**, 245–257.
15 L. Delmotte, C. Ganne-Chedeville, J. M. Leban, A. Pizzi and F. Pichelin, *Polym. Degrad. Stab.*, 2008, **93**, 406–412.
16 R. Rana, R. Langenfeld-Heyser, R. Finkeldey and A. Polle, *Wood Sci. Technol.*, 2010, **44**, 225–242.
17 G. Xu, L. Wang, J. Liu and J. Wu, *Appl. Surf. Sci.*, 2013, **280**, 799–805.
18 W. Wang, Y. Zhu, J. Cao and W. Sun, *Appl. Surf. Sci.*, 2015, **324**, 332–338.
19 G. Sinn, A. Reiterer and S. E. Stanzl-Tschegg, *J. Mater. Sci.*, 2001, **36**, 4673–4680.
20 B. Belleville, G. Koumba-Yoya and T. Stevanovic, *J. Wood Chem. Technol.*, 2019, **39**, 43–56.
21 D. Singh, J. Zeng, D. D. Laskar, L. Deobald, W. C. Hiscox and S. Chen, *Biomass Bioenergy*, 2011, **35**, 1030–1040.
22 M. Hakkou, M. Pétrissans, A. Zoulalian and P. Gérardin, *Polym. Degrad. Stab.*, 2005, **89**, 1–5.
23 L.-P. Xiao, Z.-J. Shi, Y.-Y. Bai, W. Wang, X.-M. Zhang and R.-C. Sun, *BioEnergy Res.*, 2013, **6**, 1154–1164.

24 S. F. Curling, C. A. Clausen and J. E. Winandy, *For. Prod. J.*, 2002, **52**(7/8), 34–39.
25 S. Mahapatra and D. Banerjee, *Microbiol. Insights*, 2013, **6**, MBI-S10957.
26 D. Jaros, J. Köbsch and H. Rohm, *Eng. Life Sci.*, 2018, **18**, 743–752.
27 M. H. Sugai-Guérios, W. Balmant, A. Furigo, N. Krieger and D. A. Mitchell, in *Filaments in Bioprocesses*, ed. R. Krull and T. Bley, Springer International Publishing, Cham, 2015, pp. 171–221.
28 A. Ioannou and C. Varotsis, *PLoS One*, 2017, **12**, e0188095.
29 E. M. S. Pérez, M. Ávalos, R. Babiano, P. Cintas, M. E. Light, J. L. Jiménez, J. C. Palacios and A. Sancho, *Carbohydr. Res.*, 2010, **345**, 23–32.
30 Z. Zhao, C. Huang, D. Wu, Z. Chen, N. Zhu, C. Gui, M. Zhang, K. Umemura and Q. Yong, *Ind. Crops Prod.*, 2020, **152**, 112501.
31 A. Sluiter, B. Hames, R. Ruiz, C. Scarlata, J. Sluiter, D. Templeton and D. Crocker, *Determination of structural carbohydrates and lignin in biomass*, 2008.
32 A. Sluiter, R. Ruiz, C. Scarlata, J. Sluiter and D. Templeton, *Determination of extractives in biomass*, 2005.
33 A. Sluiter, B. Hames, R. Ruiz, C. Scarlata, J. Sluiter and D. Templeton, *Determination of ash in biomass*, 2005.
34 K. Fackler, M. Schmutzer, L. Manoch, M. Schwanninger, B. Hinterstoisser, T. Ters, K. Messner and C. Gradinger, *Enzyme Microb. Technol.*, 2007, **41**, 881–887.
35 J. Santander, T. Martin, A. Loh, C. Pohlenz, D. M. Gatlin and R. Curtiss, *Microbiology*, 2013, **159**, 1471–1486.